Quaternary Geochronology 73 (2022) 101377

Contents lists available at ScienceDirect

Quaternary Geochronology

journal homepage: www.elsevier.com/locate/quageo

First high-resolution luminescence dating of loess in Western Siberia

N.E. Volvakh [a,1,*], R.N. Kurbanov [b,c], V.S. Zykina [a], A.S. Murray [e], T. Stevens [f], C.A. Költringer [f], A.O. Volvakh [a], D.G. Malikov [a], N.A. Taratunina [g], J.-P. Buylaert [d]

[a] Academician Koptyug Ave., 3, 630090, Novosibirsk, Russia
[b] A. Donish Institute of History, Archaeology and Ethnography, National Academy of Sciences of Tajikistan, ak. Rudaki ave., 33
[c] Staromonetny per., 29/4, 119017, Moscow, Russia
[d] Department of Physics, Technical University of Denmark, DTU Risø Campus, Roskilde, Denmark
[e] Nordic Laboratory for Luminescence Dating, DTU Physics and Department of Geoscience, Aarhus University, DTU Risø Campus, Roskilde, Denmark
[f] Department of Earth Sciences, Uppsala University, Uppsala, Sweden
[g] Leninskiye gory, GSP-1, Moscow, Russia

ARTICLE INFO

Keywords:
Loess-palaeosol sequence
Ob loess plateau
Late Pleistocene
Erosional hiatus
Lozhok

ABSTRACT

The south of Western Siberia is an important part of the Eurasian loess belt, containing an extensive record of Quaternary landscape and climate evolution in up to 100 m thick loess deposits with as many as 10 pedocomplexes. However, this important Quaternary archive lacks a reliable absolute chronology, and this has prevented the linking of the widely accepted regional chronostratigraphic correlations with those of other parts of the Eurasian loess belt. Here we present the first results of detailed luminescence dating of the Late Pleistocene loess-palaeosol sequence at the Western Siberian stratotype section of Lozhok. According to the classical regional chronostratigraphic scheme, this sequence records the main stages of the environmental evolution of the region, including three palaeosols correlated with the warming stages of MIS 5e, MIS 5c and MIS 3. Our absolute chronology is based on 38 new luminescence ages (OSL, IR_{50}, $pIRIR_{290}$). Good agreement between the OSL and $pIRIR_{290}$ ages suggests sufficient bleaching before deposition. The resulting chronology reveals that, rather than being only Upper Pleistocene in age, the loess-palaeosol sequence at Lozhok actually formed in the Middle and Upper Pleistocene. The ages of individual horizons do not correspond to the previously accepted stratigraphic units and morphological features of pedocomplexes. Our Bayesian chronological model reveals remarkable variation in dust accumulation and preservation at the site. The new results unambiguously identify the presence of an erosional boundary with a hiatus lasting ~90 ka. The upper pedocomplex, immediately below this discontinuity, formed in sediment deposited between 131 ± 9 ka and 122 ± 11 ka and clearly corresponds to MIS 5. The lower pedocomplex is found in sediment deposited between 240 ± 12 and 199 ± 9 ka, and correlates closely with MIS 7. These new findings demonstrate the urgent need for a wider programme to date the main stratotypes of loess-palaeosol sections in Western Siberia. Only then can the global implications of the regional climate record in this important continental-scale archive be correctly interpreted.

1. Introduction

This study aims to establish the first absolute chronology for loess in Western Siberia using the loess-palaeosol stratotype at Lozhok. Loess deposits are widely developed in the south of Western Siberia and are an important palaeoclimatic archive of the Late and Middle Pleistocene (Zykina and Zykin, 2012). In the south of Western Siberia (Fig. 1), thick loess deposits are located in the upper part of the Ob River basin and form the Ob Loess Plateau – a system of north-eastern elongated ridges which cover other Quaternary landforms. These extensive loess sequences include well-preserved fossil soils and represent some one of the most complete continental records of the Pleistocene climate in the world (Kravchinsky et al., 2008). Periodic climate fluctuations are reflected in the regular alternation of loess and automorphic soil horizons; this sedimentary sequence has developed as a direct result of differences in temperature and moisture supply through time.

The most complete loess-soil sequence in Western Siberia (Ob Loess plateau) exhibits 10 pedocomplexes (including the modern soil) within

* Corresponding author.
E-mail address: volvakh@igm.nsc.ru (N.E. Volvakh).
[1] Please see acknowledgements.

https://doi.org/10.1016/j.quageo.2022.101377
Received 15 December 2021; Received in revised form 11 July 2022; Accepted 21 July 2022
Available online 11 August 2022

the Brunhes Chron, separated by thick layers of loess. Each pedocomplex consists of soils separated by thinner loess interlayers. Although the loess-palaeosol sequences of the region have been well studied (Sizikova and Zykina, 2014, 2015; Zykin and Zykina, 2015; Zykina and Zykin, 2012; Zykina et al., 2018), no detailed chronostratigraphic studies have been undertaken. Currently the regional stratigraphic correlation of loess-palaeosol sequences from different parts of Western Siberia (Ob Loess plateau; Salair area, Novosibirsk Ob area, Altai piedmont, Yenisei loess area etc.) is based on descriptions of the palaeosols, palaeomagnetic studies, and rare TL ages. This regional scheme is ultimately correlated with the Kurtak section, one of the most complete loess-soil sections of the Upper Pleistocene of Central Siberia. There, a broad stratigraphic sequence of subaerial sedimentation and the age intervals of soil formation and loess accumulation has been suggested, based on TL dating (Frechen et al., 2005; Zander et al., 2003). A reliable numerical timescale is of great importance for the reconstruction of the palaeoenvironment from loess-palaeosol sequences (Stevens et al., 2006). Recent developments in optically or infrared stimulated luminescence dating using quartz and feldspar (e.g. Buylaert et al., 2012; Murray et al., 2021), in combination with a high sampling density (e.g. Stevens et al., 2018), is expected to allow a more robust and detailed reconstruction of the sedimentation and soil forming processes in Western Siberia. In particular, key sections such as Lozhok require detailed luminescence dating to establish independent chronostratigraphic models that do not rely on regional correlations. In this study, luminescence dating is applied to both quartz and feldspar grains extracted from thirty-eight samples from a ~8.3 m loess-palaeosol profile at Lozhok. A continuous Bayesian age-depth model is then derived from these ages, and the results interpreted in terms of the regional stratigraphic scheme and global marine oxygen isotope stages.

1.1. Site description

The Lozhok section is located in an abandoned brick-clay quarry, 1.5 km west of Lozhok railway station (54°34′02.5″N, 83°18′31.9″E) at an altitude of approximately 165 m asl (Fig. 1). The site is located in the Novosibirsk Region, at the interfluve of the Shipunikha and Koinikha rivers, tributaries of the Berd River which in turn flows into the Ob River. The section is located on the slope of one of the northern ridges of the Ob Loess Plateau, which is made up of a series of elevated elongated ridges, oriented from southwest to northeast, dissected by small river valleys (Fig. 1).

The Lozhok section was chosen for dating due to its apparent stratigraphic completeness and position as a key section of the Late Pleistocene of the entire Ob Loess Plateau. Indeed, the section has been identified as a stratotype for the Novosibirsk Ob Region (Zykina et al., 1981; Zykina and Zykin, 2012). Previously, geomorphological, stratigraphic, and palaeopedological studies (Volkov, 1971; Zykina et al., 1981; Volkov, 1973) and studies of its granulometric, geochemical, micromorphological (Sizikova and Zykina, 2014, 2015; Sizikova and Zykina, 2013), petromagnetic characteristics (Kravchinsky et al., 2008; Volvakh et al., 2019) and the morphology of quartz grains (Sizikova and Zykina, 2015) have been undertaken at the site. The presence of short-period climatic oscillations in the loess record has also been investigated based on the sedimentological properties of the loess (Sizikova and Zykina, 2015; Volvakh et al., 2019).

Based on this previous work, the section is thought to consist of five lithostratigraphic units: (1) the modern soil; (2) the Bagan-Eltsovka loess correlated to MIS 2; (3) the Iskitim palaeosol, correlated with MIS 3; (4) the Tulino loess - MIS 4 and (5) the Berd pedocomplex, with one weakly developed and one thick palaeosol, both correlated with MIS 5. This interpretation is based on radiocarbon ages from both Lozhok and the nearby Mramorny quarry. The Iskitim palaeosol of Southern Siberia is correlated with MIS 3 and in some sections consists of two separate weakly developed soils. The lower soil was dated to 33–38 ka cal BP and the upper palaeosol to 26–30 ka cal. BP (Zykina et al., 1981; Volkov, 1973).

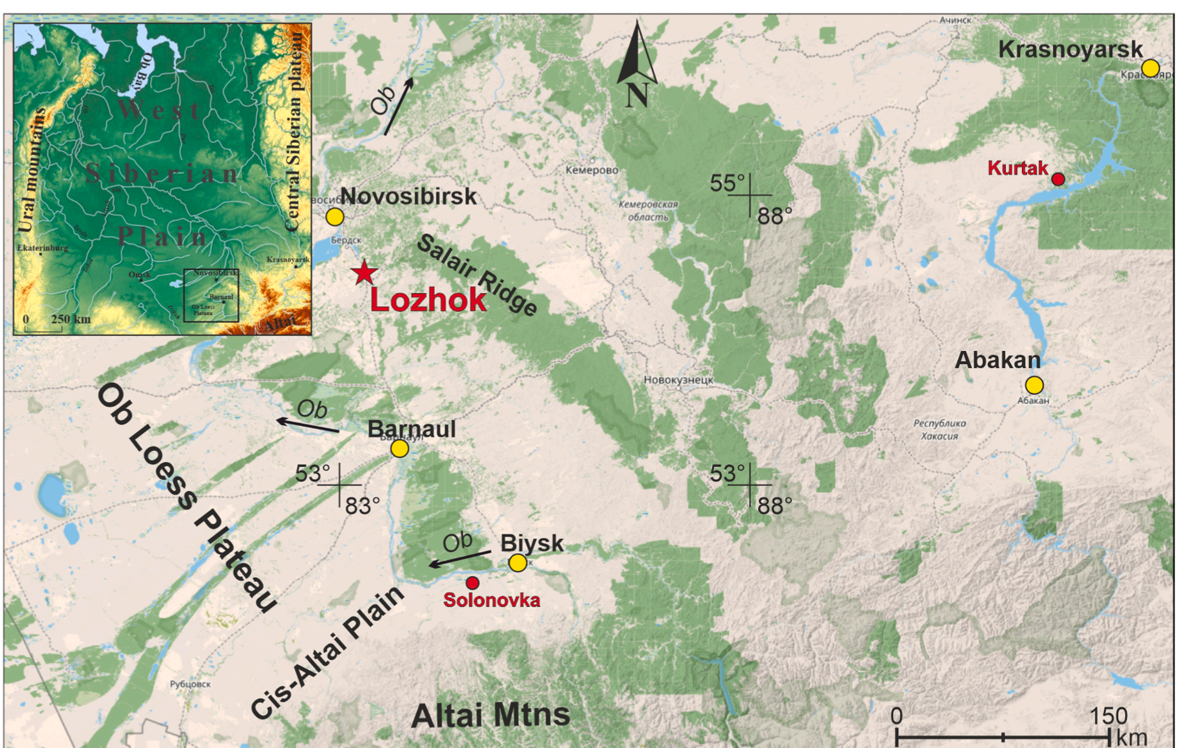

Fig. 1. Location of the Lozhok section (DEM from OpenStreetMap).

2. Material and methods

In this study, 40 luminescence samples were collected from the ~8.3 m thick loess profile at Lozhok. Samples were collected in light-proof bags after sunset immediately after cleaning back of the section. Samples for gamma spectrometry were taken separately around the luminescence samples. The sampling scheme is outlined in Fig. 2.

The 90–180 μm grains for measuring the equivalent dose were obtained by wet sieving, followed by treatment with 10% H_2O_2, 10% HCl and 10% HF. This was followed by separation of quartz grains and K-rich feldspar grains in a heavy liquid solution (sodium polytungstate) of density 2.58 g/ml. The quartz-rich extract was etched in 40% HF (40 min) and given a final wash in 10% HCl. This removed any remaining feldspar contamination, and etched the surface of the quartz grains. Two samples (186170 and 186,172) did not yield sufficient 90–180 μm grains and were discarded from analyses.

For the determination of the environmental dose rate the sediment was first dried at 50 °C, ground (<200 μm) and ignited at 450 °C for 24 h to eliminate organic matter (typically 2–3% by weight). The fine powder was mixed with a hot wax and poured in a cup-shaped mould. Finally, the radionuclide concentrations (expressed in terms of dry weight of sample before ignition) were determined by analyzing the cups on a high-resolution gamma spectrometer (Murray et al., 1987, 2018). Field water content was measured directly on the samples and ranged from 10 to 15%.

Quartz grains were mounted as large (8 mm) aliquots on stainless steel discs and K-rich feldspar grains as small (2 mm) aliquots in stainless steel cups. Quartz D_e values were measured using a standard SAR protocol (Murray and Wintle, 2003): preheat 260 °C/10s, cut-heat 220 °C, sample temperature/duration during stimulation 125 °C for 40s, and at the end of each cycle an elevated temperature blue light stimulation (40s) at 280 °C. Net signals used in further calculations were derived from the photon sum during the first 0.8s minus that in the subsequent 0.8 s. The quartz purity was checked by the absence of a significant IRSL

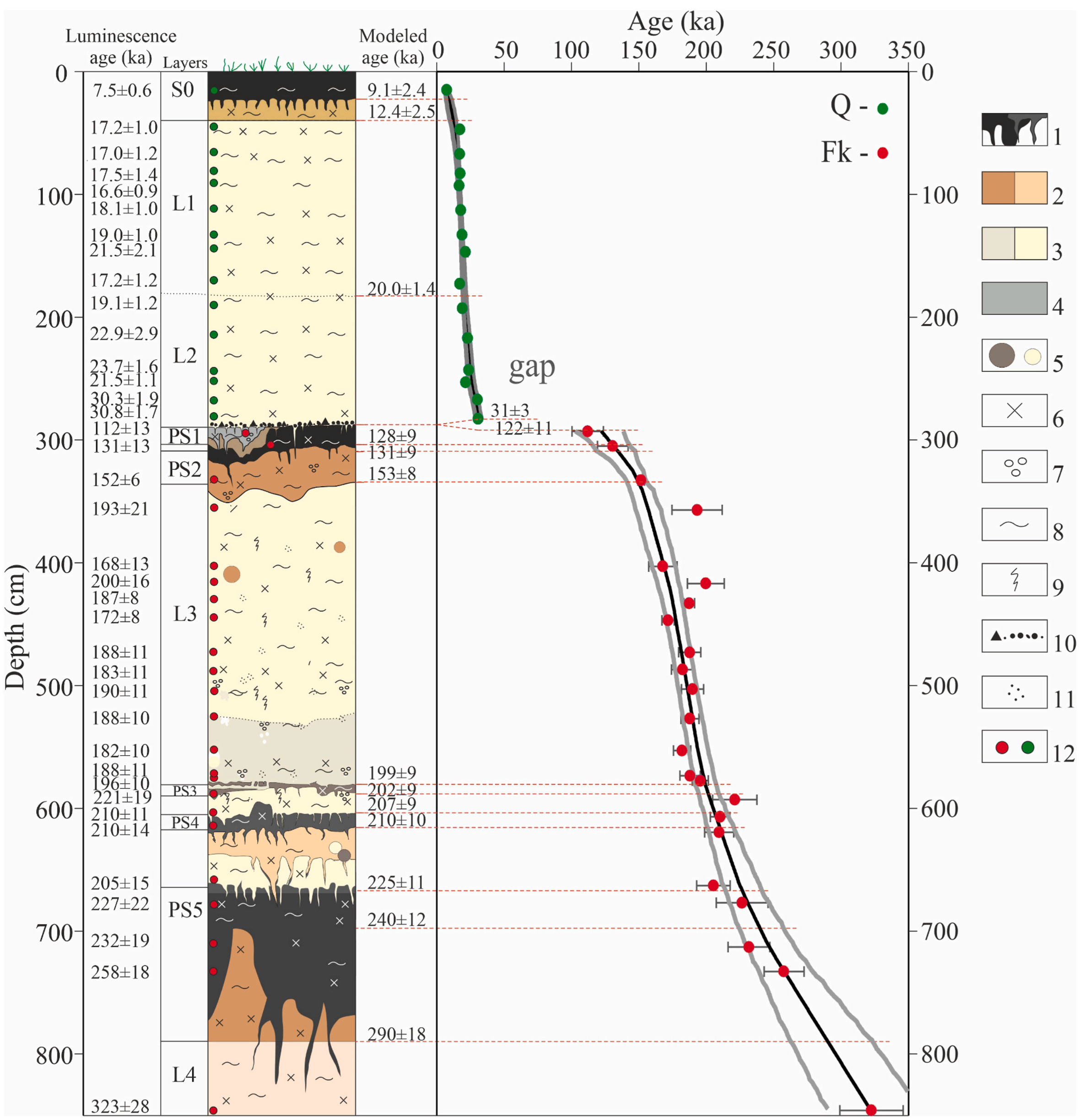

Fig. 2. Structure of the Lozhok section, showing luminescence ages and results of Bayesian modelling. Legend: 1 – humus horizon; 2 – illuvial horizon; 3 – loess horizon; 4 – sandy loam palaeosol horizon; 5 – crotovinas; 6 – secondary carbonates; 7 – gleying; 8 – loam; 9 – ferruginization; 10 – small rock debris and sand interlayer; 11 – manganese dots; 12 – sampling place.

signal (<10% of blue-light stimulated luminescence). At least 17 aliquots were measured for each quartz sample, and 6 for each feldspar sample. Feldspar measurements were performed using post-IR IRSL protocols that have been successfully applied to loess from China and Europe ($pIRIR_{50,290}$ and $pIRIR_{200,\,290}$) (Buylaert et al., 2012; Thiel et al., 2011; Stevens et al., 2018). Preheats for dose and test dose were always 320 °C for 60s, infra-red stimulation was for 200 s and at the end of each SAR cycle the feldspar signal was cleaned using IR-stimulation at 325 °C. The test dose size was ~30% of the measured D_e. For the upper part of the sequence (samples 186,151 to 186,165), the first IR stimulation was conducted at 50 °C whereas the older samples (186166–186,190) the first IR stimulation was done at 200 °C; the latter giving a more stable signal for older samples (see Li and Li, 2012; Buylaert et al., 2012; Yi et al., 2015). Luminescence from the first 2 s and from the last 20 s of the stimulation curves were used for signal and background, respectively. The results of dose recovery tests (see below) justify our choice of protocols. All measurements were performed on Risø TL/OSL-readers (model DA-20) equipped with a calibrated $^{90}Sr/^{90}Y$ beta source (Bøtter-Jensen et al., 2010; Hansen et al., 2015). For dose recovery experiments, quartz aliquots were bleached at room temperature under blue light in the reader (100s stimulation, 10 ks pause, 100s stimulation), feldspar aliquots were bleached for 48 h in a Dr Hönle solar simulator.

3. Results

3.1. Loess-palaeosol stratigraphic interpretation

Detailed layer-by-layer descriptions of the section have been published before in a number of papers (e.g. Sizikova and Zykina, 2015, 2014; Zykina et al., 1981) and are only summarised here. The initial results of the luminescence dating (15 ages) were presented in (Volvakh et al., 2021), without supporting information. Here the quartz and feldspar luminescence characteristics and full chronology (38 ages) are presented.

In our excavation the following stratigraphic units were distinguished (from bottom to top) (Fig. 2):

- layer 8 (L4) – Light brown dense loess visible from 7.8 m downwards; upper part affected by the infiltration of cracks filled with the material from PS5. In the regional stratigraphic scheme this is believed to correspond to the Suzun loess unit (MIS 6).
- layer 7 (PS3, PS4 and PS5) - Berd pedocomplex, represented in the section by 2 well developed buried soils (PS 4 and PS5) and one weakly developed palaeosol (PS3) (5.4–7.8 m). The upper well developed Berd soil (PS4; 5.8–6.1 m) consists of a humic A (5.8–5.9 m) and BC horizons (5.9–6.1 m). The lower palaeosol (PS5; 6.3–7.8 m) is represented by two horizons: A (6.3–7.6 m) and B (7.6–7.8 m). In PS3 a minor increase in organic matter and darkened colour was recorded. In the regional stratigraphic scheme, this pedocomplex is considered to be the MIS 5 stratotype for Southern Siberia (Berd pedocomplex of Kazantsevo stage), with the upper well developed soil correlated with substage MIS 5c and the lower soil with MIS 5e.
- layer 6 (L3) – Light brown silty loess with small carbonate concretions and krotovinas in the upper part (3.4–5.4 m). This is considered to represent the Tulino loess unit (MIS 4) in the regional stratigraphic scheme. At the base of the layer an embryonic soil has been identified from differences in texture and organic matter enrichment (PS3).
- layer 5 (PS2) – The lower palaeosol of the Iskitim pedocomplex (2.85–3.4 m). It consists of a humic horizon A (2.85–3.1 m) and a BC horizon (3.1–3.4 m). This pedocomplex is traditionally correlated with the first half of MIS 3 under the prevailing regional model.
- layer 4 (PS1) – the upper palaeosol of the Iskitim pedocomplex is comprised of a sandy, gleyed gray loam that is dissected by small permafrost wedges. Along the upper boundary there is an interlayer of sandy loam with inclusions of a large amount of small pebbles, gravel and grus. Field studies clearly show an erosional boundary between the Iskitim pedocomplex and the Bagan-Eltsovka loess marked by a sharp transition from soil to loess and a sandy interlayer between two units with gravel. PS1 is only represented in some parts of the sequence and the top part of this soil is often eroded.
- layer 3 (L2) – Pale silty loess, with rare black spots of organic matter (1.9–2.85 m). Under the regional stratigraphic scheme this unit is correlated with Eltsovka loess unit (second half of MIS 3).
- layer 2 (L1) – Pale loess, porous, with carbonate concretions (0.5–1 cm), homogeneous between 0.9 and 1.9 m. This unit is distinguished from L2 by growth in carbonate content and porosity. In the stratigraphic chart of Southern Siberia, this unit is correlated with Bagan loess unit (MIS 2).
- layer 1 (S0) - modern soil (0–0.9 m), comprising a humic A horizon (0–0.25 m), B1 horizon (0.25–0.55 m) and B2ca horizon (0.55–0.9 m).

3.2. Dose rate

Dose rates were calculated from gamma-spectrometry activity measurements using conversion factors from Guérin et al. (2012), with the results given in Table S1. The measured concentrations of ^{226}Ra, ^{232}Th and ^{4}K are typical for loess: ^{226}Ra is in the range of 30–40 Bq/kg, ^{232}Th - 30–40 Bq/kg, ^{4}K - 500–550 Bq/kg. Sample 186190 from the Suzun loess horizon is distinguished by low activity which may reflect a change of source material. With the exception of this lowermost sample (186190, with a lower dose rate) total dose rates do not vary significantly across the section. Average values lie around 2.5–3.0 Gy/ka for quartz and 3.0–3.9 Gy/ka for K-rich feldspars (the latter has an internal beta dose rate of 0.56 ± 0.03 Gy/ka, based on an assumed 12.5% K concentration).

Estimation of lifetime water contents for these sediments was carried out on the basis of the average particle size and the proximity of the groundwater. Lozhok section is not affected by local rivers and the groundwater level is currently low; this is not expected to have been higher during the Late Quaternary. Data on the granulometric composition of the main horizons made it possible to differentiate typical likely water contents based on the clay fraction proportion. For samples with a fraction of <2 μm in the range 12.5–17% (mainly palaeosols), a best estimate of the life-time average water content is ~15% (50% of measured saturation values) while for the other (mainly unaltered loess) samples it lies at ~10% (30% of measured saturation values). These values are consistent with the range of observed field water contents (see above).

3.3. Quartz OSL characteristics

The quartz OSL signal is dominated by a fast component (Fig. 3a) and reliable interpolation of natural signals onto the laboratory dose response curve is possible at least up to ~100 Gy (Fig. 3b). A dose recovery test was conducted on nine samples (186151–186157, 186160 and 186163) with given doses close to the estimated natural. The average dose recovery ratio obtained from these samples is 1.02 ± 0.02 (n = 43), demonstrating that we can use our chosen protocol to make reliable quartz OSL estimates of a dose administered before any heating of the sample. The measured doses are plotted as a function of the given doses in Fig. S1. The calculated D_e values for all samples are presented in Table S2. Measurements for quartz were made for nearly all the samples down to a depth of ~430 cm, but starting from sample 186165 the signals are in full saturation and only feldspar ages are considered (next section).

3.4. Feldspar luminescence characteristics

A typical K-rich feldspar $pIRIR_{200,290}$ natural test dose (277 Gy) decay and laboratory dose response are shown in Fig. 3c and d for

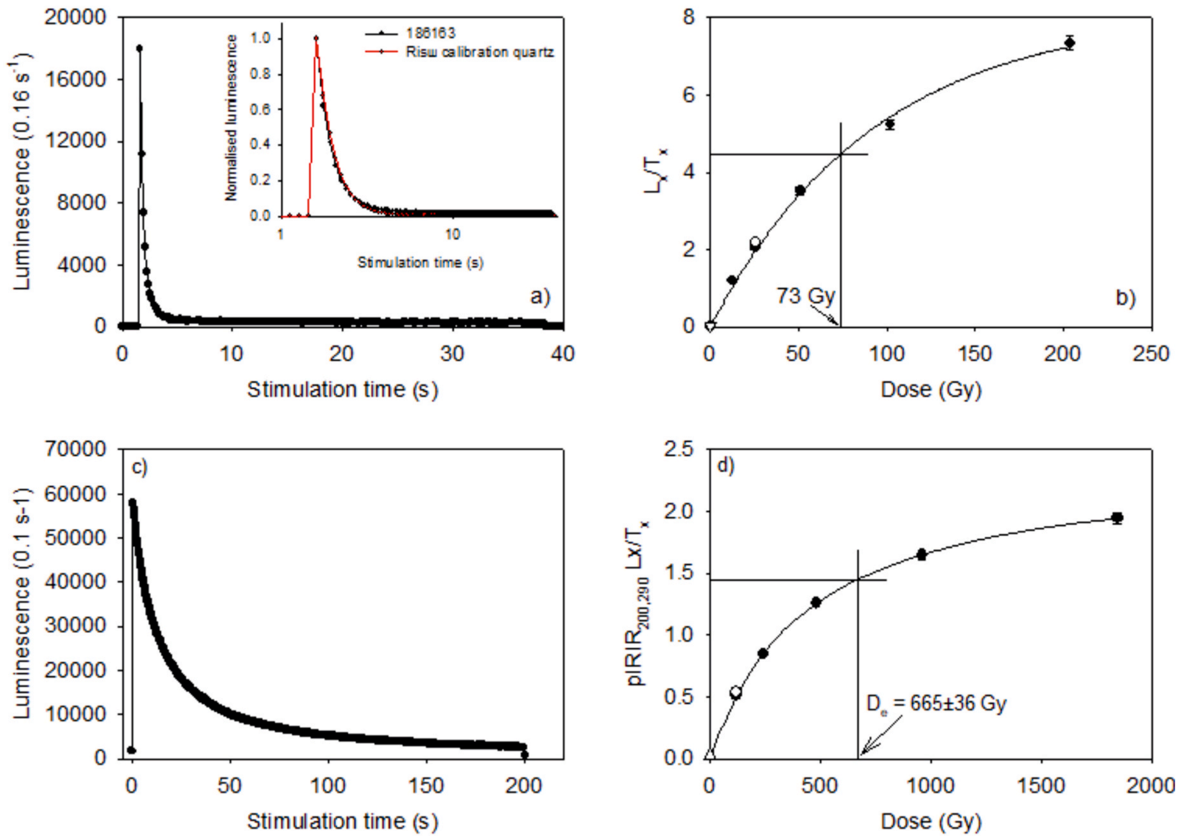

Fig. 3. Example luminescence characteristics for samples from Lozhok: a-b – Quartz OSL natural test dose (8.3 Gy) decay curve (a) and dose response curve (b) for sample 186163; c-d – K-feldspar $pIRIR_{200,290}$ natural test dose (277 Gy) decay curve (a) and dose response curve for sample 186182. Recycling ratios are shown as open circles and zero dose response (recuperation) as open triangles.

sample 186182. Dose recovery tests were applied to samples 186152, 186155 and 186157 for $pIRIR_{50,290}$ and to 186167 and 186180 for $pIRIR_{200,290}$ protocols. Sets of aliquots (at least 6 per sample) were bleached in the solar simulator for 48 h. One set of aliquots was given a dose close to natural dose and another set of aliquots was used to estimate residual dose. For the $pIRIR_{50,290}$ protocol the given dose ranged between 61 and 78 Gy and the measured residuals from 4.4 ± 1.6 Gy to 15.0 ± 0.4 Gy. After subtracting the residual dose the average measured to given dose ratio is 0.93 ± 0.02 (n = 12). For the $pIRIR_{200,290}$ protocol the given doses were 391 and 684 Gy for samples 186167 and 186180, respectively. Measured residuals were 41 ± 2 Gy and 47 ± 2 Gy, respectively. After subtracting the measured residual dose the average measured to given dose ratio for the $pIRIR_{200,290}$ protocol is 1.01 ± 0.05 (n = 6). These results suggest that we can use our chosen $pIRIR_{290}$ SAR protocols to make reliable feldspar IRSL estimates of a dose administered before any heating of the sample. The K-rich feldspar D_e estimates ($pIRIR_{50,290}$ for samples 186151-186166 and $pIRIR_{200,290}$ for samples 186167-186190) are arithmetic averages following Guérin et al. (2017), and are given in Table S2 with no residual subtraction.

3.5. Comparison of quartz OSL and K-rich feldspar $pIRIR_{290}$ ages and age modelling

The quartz OSL ages ranged from 7.5 ± 0.7 ka for the youngest sample to 30.8 ± 1.9 ka for the oldest datable sample. The K-rich feldspar $pIRIR_{290}$ ages increase systematically from 10.1 ± 0.8 ka to 326 ± 28 ka and are broadly in stratigraphic order. The $pIRIR_{290}$ ages are plotted against the available quartz OSL ages in Fig. 4. The $pIRIR_{290}$ ages are in good agreement with the quartz OSL ages, if the offset of ~2 ka (intercept on y-axis) is taken into account. This suggests relatively complete bleaching of the $pIRIR_{290}$ signal. Based on these results, we use

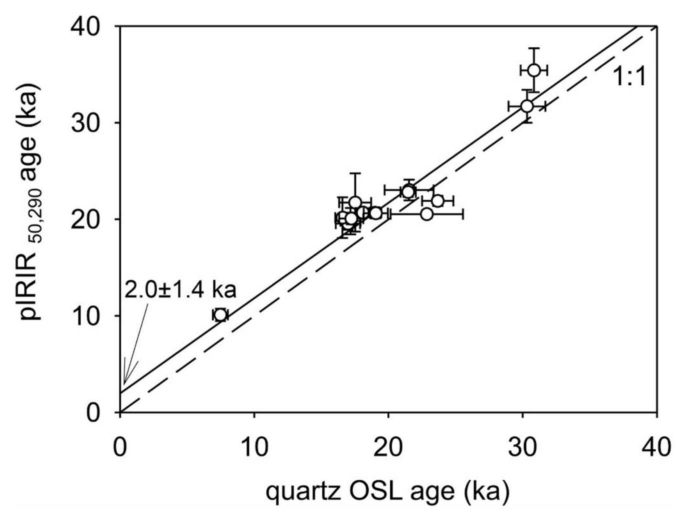

Fig. 4. Feldspar $pIRIR_{50,290}$ ages plotted as a function of quartz OSL ages for samples <30 ka old. Dashed line is drawn at unity and the solid line has a slope of 0.987 ± 0.082 and y-axis intercept of 1.96 ± 1.43 ka.

quartz OSL ages for young samples (<30 ka) and K-rich feldspar $pIRIR_{290}$ ages for older samples. From the feldspar/quartz age intercept (2.0 ± 1.4 ka) we calculate an average residual dose in the field of 7 ± 5 Gy (taking the average feldspar dose rate); this was subtracted from the feldspar D_e values listed in Table S2 before final age calculation and age-depth modelling.

For modelling, the systematic uncertainty component arising from beta source calibration, water content, internal dose rate from U/Th, and cosmic ray component was removed from the quartz OSL and feldspar $pIRIR_{290}$ age uncertainties. Then a Bayesian model was run on the accepted ages as outlined above using rBacon software (Blaauw and Christeny, 2011) available as an R package, to give an age-depth model at 1 cm interval for the section. The age gap in the section at 285 cm meant that two separate age models were constructed and then combined (Fig. 2), with settings of acc. mean = 600 and thick = 16 for the lower part and acc. mean = 200 and thick = 8 for the upper part of the section. Finally an average systematic uncertainty was combined with the random uncertainties given by the Bayesian model, to give total uncertainties on modelled ages.

4. Discussion

The new chronology at Lozhok, based on our Bayesian model, shows that much of the lower part of the sequence at Lozhok is far older than previously believed based on the regional stratigraphic model for the Ob loess plateau. In order to correlate this age model with field observations, we must consider the subdivision into palaeosol and loess units more carefully. Apart from some obvious and limited cryoturbation, the upper boundaries of palaeosols are well defined, and correspond to the field definitions. However, there is no doubt that during formation, soils penetrate down into the older loess deposited during the previous cold period (Stevens et al., 2007), particularly in the presence of permafrost. This is especially obvious at the bottom of PS5, but is also observed to a lesser extent at the bottom of all palaeosol layers. For this reason, one cannot assume that a pedologically defined boundary (e.g. between PS5 and L4) defines the surface at the time of a change from cold/dry to warm/wet climate – such a change must have actually occurred when the surface was significantly more elevated. Accordingly, we associate the more elevated point in the altered loess of PS5 (see horizontal dashed red line at 698 cm in Fig. 2) with the lower limit of the presumed sediment surface at the time of the beginning of significant soil formation. Similar dashed red lines connecting the stratigraphic section with the age model are drawn in the lower part of all palaeosol units (at PS4 - 616 cm, PS3 - 589 cm, PS2 - 305, cm PS1 - 301 cm, S0 - 23 cm); other red dashed lines are drawn at the same elevation as the field defined unit boundaries. The corresponding modelled age is written adjacent to each of these red lines.

We are now in a position to discuss the relationship between the stratigraphy and the age model. A single pIRIR age of 332 ± 28 ka was obtained at the base of the section from the L4 (Suzun) loess. The L4 loess becomes visibly altered about 790 cm (modelled age 290 ± 18 ka), and the sediment containing PS5 (lowest unit in the Berd pedocomplex) was deposited between 240 ± 12 and 225 ± 11 ka. PS5 is separated from the upper well-developed PS4 by a thin layer of loess, and the PS4 palaeosol is found in sediment deposited from 210 ± 10 to 207 ± 9 ka. Thus we conclude that the L4 Suzun loess unit formed during MIS 8, while the Berd pedocomplex, formed between 240 ± 12 and 207 ± 9 ka, correlates with the MIS 7 interglacial. This contrasts with the previous MIS 6 and 5 assignment. At the top of Berd pedocomplex, an embryonic soil has been identified (PS3); this has not been discussed before in the literature and has an age of 200 ± 9 ka, with an underlying thin loess unit above PS4. The upper part of this complex is therefore consistent with a late MIS 7 formation, and may indicate formation during the substage MIS 7a.

The L3 (Tulino) loess began to deposit at 199 ± 9 ka, and continued until 131 ± 9 ka. Thus the entire MIS 6 appears to be represented. Apparent accumulation may have decreased towards the end of MIS 6. This may have been a result of deflation, consistent with the evidence of apparent cryogenic processes in the loess deposited after ~150 ka.

The humus horizon of the lower Iskitim palaeosol (PS2) formed in sediment deposited between 131 ± 9 and 128 ± 9 ka; the underlying BC horizon penetrates down into sediment deposited from 153 ± 8 ka (341 cm). We correlate this PS2 palaeosol with the MIS substage 5e, with the BC horizon developed into underlying MIS 6 loess. Above PS2 a gley soil (PS1) formed in sediment deposited between 128 ± 9 and 122 ± 11 ka, pointing to continued development in MIS 5. However, these soils are truncated by a clear erosional boundary marking a hiatus in sedimentation at a depth of 290 cm, clearly visible in the field. This is confirmed by the ages, which indicate an age discontinuity of ~90 ka, with loess immediately above the unconformity dated to 31 ± 3 ka. Thus, material formed during most of MIS 5, and all of MIS 4 and MIS3 is missing. It has presumably been removed, probably by slope erosion given that the site is located near the edge of a loess hill. While the erosional boundary is recognisable in the field, its duration only becomes clear as a result of the new chronology.

The formation of the Eltsovka-Bagan loess (L2-L1) took place during a period of significant atmospheric dust accumulation between ~31 ± 3 and ~9.1 ± 2.4, although the loess deposited after 12.4 ± 2.5 ka has been altered by Holocene soil formation. The ages show a relatively continuous process of loess accumulation. This accumulation may have been more rapid between ~25 and 14 ka (see also Fig. S1), corresponding to peak last glacial conditions, and coinciding with a peak in dust accumulation in loess sequences across the Northern Hemisphere. In the stratigraphic scheme of South Western Siberia, the Suminskaya palaeosol is identified as present between the Eltsovka-Bagan (L2-L1) loess layers; its age has been estimated at 19–16.6 ka (Zykina et al., 1981). If we have correctly identified the L2-L1boundary in our section, our model suggests an age of 20.0 ± 1.4, consistent with the older end of the age range suggested by Zykina et al. (1981). This palaeosol is not found at the Lozhok section, and the continuous chronology here indicates that it was most likely not removed. Presumably the rate of dust accumulation was large enough to mask or prevent any soil formation at that time. More generally, the OSL ages confirm the accumulation of the Eltsovka-Bagan loess during MIS 2 and they correlate with the age of the regional Sartan glaciation (Volvakh et al., 2021). The Holocene soil S0 is found in loess that deposited from 9.1 ± 2.4 ka.

Overall, our new chronostratigraphy based on a detailed luminescence dating of the Lozhok stratotype section demonstrates that the previous understanding of the age of the sequence is incorrect. Rather than the whole exposure being Upper Pleistocene, only the upper part of the sequence formed during this period and a large part of the sediments from MIS 5 to 3 (~90 ka) is missing, presumably removed by erosion. The underlying sediments were formed in the Middle Pleistocene, and, given the many published correlations with other sections across Siberia, it seems likely that similar undetected gaps may be found elsewhere. The very high accumulation rates at Lozhok during MIS 2 show that dust accumulation in the Ob loess plateau responded to, or occurred at the same time as, the wider, hemispheric climate forcing that lead to substantially increased dustiness over this interval over the Northern Hemisphere, particularly from 25–20 ka. Rapid loess accumulation is also seen in the section during MIS 6 (Tulino loess). In general, sediment accumulation rates are lower in the interglacial soil horizons, as would be expected, but these are not uniform (or not uniformly preserved) in glacial stages. Accumulation at the site is characterised by periods of intense, rapid loess deposition, punctuated by longer phases with little accumulation, or perhaps shorter periods of erosion. To what extent this characterises other sections in Western Siberia requires testing.

5. Conclusion

Quartz OSL and K-feldspar $pIRIR_{290}$ dating has been applied to thirty-eight samples of quartz and feldspar extracted from the Lozhok loess-palaeosol sequence, providing the first detailed luminescence chronology for Western Siberian loess. The age estimates indicate that the loess-soil sediments of the Lozhok section, previously considered to be Upper Pleistocene, were actually formed in the Upper and Middle Pleistocene. Moreover, the age of all the units older than ~30 ka do not agree with the accepted stratigraphic chart for Southwestern Siberia. Our results show that the erosional boundary identified at a depth of 3 m represents a significant depositional hiatus of about 90 ka; clearly a significant part of the Late Pleistocene geological record is missing in the Lozhok section. The Iskitim palaeosol complex (PS1 and PS2), Tulino loess (L3) and Berd pedocomplex (PS4 and PS5), are significantly older than the previously accepted stratigraphy of this section. The lower PS5, described as a typical palaeosol of Kazantsevo interglacial and previously correlated with MIS 5e, in fact correlates with MIS 7. The underlying and overlying loess units of the pedocomplex belong to MIS stages 8 and 6, respectively. The upper palaeosol (PS2) previously correlated with MIS 3 corresponds to MIS 5e. This re-evaluation of the stratotype section at Lozhok has major implications for our understanding of Middle to Late Pleistocene loess sedimentation and climate change throughout Siberia, and testing of whether these results are representative of the regional record is urgently required. These new data also hint at highly variable rates of dust accumulation at the site, being particularly intense during early MIS 6 and mid to late MIS 2. If found elsewhere, this would have implications for our understanding of dust generation across Southern Siberia.

Declaration of competing interest

The authors declare that they have no known competing financial interests or personal relationships that could have appeared to influence the work reported in this paper.

Acknowledgements

N.E. Volvakh, R.N. Kurbanov, V.S. Zykina, A.O. Volvakh, D.G. Malikov, and N.A. Taratunina have removed their academic affiliation because sanctions following the Ukraine-Russian conflict prevent Danish researchers (J.-P. Buylaert, A.S. Murray) publishing with Russian state institutions. We are thankful to V.S. Zykin, A.V. Panin, M. Frechen, S. Markovich and I. Zolnikov for detailed discussion of our results.

Work is done on state assignment project № 1021051402679-4-1.5.1. This study was funded by grants № 19-35-90040, № 20-05-00801 and № 19-05-00513; R.N. Kurbanov was supported by program № 0148-2019-0005; N.A. Taratunina was supported by program № 121051100135–0.

Appendix A. Supplementary data

Supplementary data to this article can be found online at https://doi.org/10.1016/j.quageo.2022.101377.

References

Blaauw, M, Christeny, J.A., 2011. Flexible paleoclimate age-depth models using an autoregressive gamma process. Bayesian Anal. 6 (3), 457–474. https://doi.org/10.1214/11-BA618.

Bøtter-Jensen, L., Thomsen, K.J., Jain, M., 2010. Review of optically stimulated luminescence (OSL) instrumental developments for retrospective dosimetry. Radiat. Meas. 45, 253–257. https://doi.org/10.1016/j.radmeas.2009.11.030.

Buylaert, J.-P.P., Jain, M., Murray, A.S., Thomsen, K.J., Thiel, C., Sohbati, R., 2012. A robust feldspar luminescence dating method for Middle and Late Pleistocene sediments. Boreas 41, 435–451. https://doi.org/10.1111/j.1502-3885.2012.00248.x.

Frechen, M., Zander, A., Zykina, V., Boenigk, W., 2005. The loess record from the section at Kurtak in Middle Siberia. Palaeogeogr. Palaeoclimatol. Palaeoecol. 228, 228–244. https://doi.org/10.1016/j.palaeo.2005.06.004.

Guérin, G., Mercier, N., Nathan, R., Adamiec, G., Lefrais, Y., 2012. On the use of the infinite matrix assumption and associated concepts: a critical review. Radiat. Meas. 47, 778–785. https://doi.org/10.1016/j.radmeas.2012.04.004.

Guérin, G., Christophe, C., Philippe, A., Murray, A.S., Thomsen, K.J., Tribolo, C., Urbanova, P., Jain, M., Guibert, P., Mercier, N., Kreutzer, S., Lahaye, C., 2017. Absorbed dose, equivalent dose, measured dose rates, and implications for OSL age estimates: introducing the Average Dose Model. Quat. Geochronol. 41, 163–173. https://doi.org/10.1016/j.quageo.2017.04.002.

Hansen, V., Murray, A., Buylaert, J.-P., Yeo, E.-Y., Thomsen, K., 2015. A new irradiated quartz for beta source calibration. Radiat. Meas. 81, 123–127. https://doi.org/10.1016/j.radmeas.2015.02.017.

Kravchinsky, V.A., Zykina, V.S., Zykin, V.S., 2008. Magnetic indicator of global paleoclimate cycles in Siberian loess–paleosol sequences. Earth Planet Sci. Lett. 265, 498–514. https://doi.org/10.1016/j.epsl.2007.10.031.

Li, B., Li, S., 2012. A reply to the comments by Thomsen et al. on "Luminescence dating of K-feldspar from sediments: a protocol without anomalous fading correction. Quat. Geochronol. 8, 49–51.

Murray, A.S., Wintle, A.G., 2003. The single aliquot regenerative dose protocol: potential for improvements in reliability. Radiat. Meas. 37, 377–381. https://doi.org/10.1016/S1350-4487(03)00053-2.

Murray, A.S., Marten, R., Johnston, A., Martin, P., 1987. Analysis for naturally occurring radionuclides at environmental concentrations by gamma spectrometry. J. Radioanal. Nucl. Chem. Artic. 115, 263–288. https://doi.org/10.1007/BF02037443.

Murray, A.S., Helsted, L.M., Autzen, M., Jain, M., Buylaert, J.P., 2018. Measurement of natural radioactivity: calibration and performance of a high-resolution gamma spectrometry facility. Radiat. Meas. 120, 215–220. https://doi.org/10.1016/j.radmeas.2018.04.006.

Murray, A., Arnold, L.J., Buylaert, J.-P., Guérin, G., Qin, J., Singhvi, A.K., Smedley, R., Thomsen, K.J., 2021. Optically stimulated luminescence dating using quartz. Nat. Rev. Methods Prim. 1, 72. https://doi.org/10.1038/s43586-021-00068-5.

Sizikova, A.O., Zykina, V.S., 2013. Upper Pleistocene loess of the Lozhok reference section (southern West Siberia), environmental and climate dynamics. Proceedings of Altai State University, Biological Sciences, Earth Sciences Series 3-2 (79), 132–137. https://doi.org/10.14258/izvasu(2013)3.2-28.

Sizikova, A.O., Zykina, V.S., 2014. Sand quartz grain morphoscopy and micromorphology of Late Pleistocene loess layers of south os West Siberia, Lozhok section. Geol. Miner. Resour. Sib. 170, 41–50.

Sizikova, A.O., Zykina, V.S., 2015. The dynamics of the late Pleistocene loess formation, Lozhok section, Ob Loess plateau, SW Siberia. Quat. Int. 365, 4–14. https://doi.org/10.1016/j.quaint.2014.09.030.

Stevens, T., Armitage, S.J., Lu, H., Thomas, D.S.G., 2006. Sedimentation and diagenesis of Chinese loess: implications for the preservation of continuous, high-resolution climate records. Geology 34, 849. https://doi.org/10.1130/G22472.1.

Stevens, T., Thomas, D.S.G., Armitage, S., Lunn, H., Lu, H., 2007. Reinterpreting climate proxy records from late Quaternary Chinese loess: a detailed OSL investigation. Earth Sci. Rev. 80, 111–136. https://doi.org/10.1016/j.earscirev.2006.09.001.

Stevens, T., Buylaert, J.-P., Thiel, C., Újvári, G., Yi, S., Murray, A.S., Frechen, M., Lu, H., 2018. Ice-volume-forced erosion of the Chinese Loess Plateau global Quaternary stratotype site. Nat. Commun. 9, 983. https://doi.org/10.1038/s41467-018-03329-2.

Thiel, C., Buylaert, J.-P., Murray, A., Terhorst, B., Hofer, I., Tsukamoto, S., Frechen, M., 2011. Luminescence dating of the Stratzing loess profile (Austria) – testing the potential of an elevated temperature post-IR IRSL protocol. Quat. Int. 234, 23–31. https://doi.org/10.1016/j.quaint.2010.05.018.

Volkov, I.A., 1971. Late Quaternary Subaerial Formation. Nauka press, Moskow, p. 255.

Volvakh, A.O., Volvakh, N.E., Smolyaninova, L.G., 2019. Pleoclimatic changes and short-period events of the Late Pleistocene in the record of loess sediments of the Lozhok section, South-Western West Siberia. Geol. Miner. Resour. Sib. 4, 17–27. https://doi.org/10.20403/2078-0575-2019-4-17-27.

Volkov, I.A., 1973. Paleogeographic significance of some radiocarbon dates in southern West Siberia. Geol. Geophys. 2, 3–8.

Volvakh, N.E., Kurbanov, R.N., Volvakh, A.O., Zykina, V.S., Khashchevskaya, D.E., Buylaert, J.-P., Murray, A.S., 2021. The first results of luminescent dating of loess-paleosol series in the south of Western Siberia (Lozhok reference section). Izvestiya Rossiiskoi Akademii Nauk Seriya Geograficheskaya 85, 284–301. https://doi.org/10.31857/S2587556621020151.

Volvakh, A.O., Volvakh, N.E., Ovchinnikov, I.Y., Smolyaninova, L.G., Kurbanov, R.N., 2021. Loess-paleosol record of MIS 3 - MIS 2 of north-east Cis-Salair plain, south of West Siberia. Quat. Int. 620, 58–74. https://doi.org/10.1016/j.quaint.2021.06.026.

Yi, S., Buylaert, J.-P., Murray, A.S., Thiel, C., Zeng, L., Lu, H., 2015. High resolution OSL and post-IR IRSL dating of the last interglacial–glacial cycle at the Sanbahuo loess site (northeastern China). Quat. Geochronol. 30, 200–206. https://doi.org/10.1016/j.quageo.2015.02.013.

Zander, A., Frechen, M., Zykina, V., Boenigk, W., 2003. Luminescence chronology of the upper Pleistocene loess record at Kurtak in M iddle Siberia. Quat. Sci. Rev. 22, 999–1010. https://doi.org/10.1016/S0277-3791(03)00034-9.

Zykin, V.S., Zykina, V.S., 2015. The Middle and late Pleistocene loess-soil record in the Iskitim area of Novosibirsk Priobie, south-eastern west Siberia. Quat. Int. 365, 15–25. https://doi.org/10.1016/j.quaint.2014.07.011.

Zykina, V.S., Volvakh, A.O., Zykin, V.S., Volvakh, N.E., 2018. Structural features of the Upper-Pleistocene loess-soil sequence of the Kolyvan knap in the Predaltai plain. Geol. Miner. Resour. Sib. 3, 54–64. https://doi.org/10.20403/2078-0575-2018-3-54-64.

Zykina, V.S., Zykin, V.S., 2012. Loess-soil Sequence and Evolution of Paleoenvironment and Climate of West Siberia during the Pleistocene. Geo, Novosibirsk, p. 476.

Zykina, V.S., Volkov, I.A., Dergacheva, M.I., 1981. Upper Quaternary Deposits and Fossil Soils of Novosibirsk Priobie. Nauka press, Moskow, p. 204.